

Article

# Hydraulic Properties of Forest Soils with Stagnic Conditions

Stefan Julich <sup>1,\*</sup> , Janis Kreiselmeier <sup>1,2,3</sup> , Simon Scheibler <sup>1</sup>, Rainer Petzold <sup>4</sup>, Kai Schwärzel <sup>2,3</sup>  and Karl-Heinz Feger <sup>1</sup> 

<sup>1</sup> Institute of Soil Science and Site Ecology, Technische Universität Dresden, 01069 Dresden, Germany; janis.kreiselmeier@thuenen.de (J.K.); simon.scheibler@mailbox.tu-dresden.de (S.S.); karl-heinz.feger@tu-dresden.de (K.-H.F.)

<sup>2</sup> Institute for Integrated Management of Material Fluxes and of Resources (UNU-FLORES), United Nations University, 01067 Dresden, Germany; kai.schwaerzel@thuenen.de

<sup>3</sup> Thünen Institute of Forest Ecosystems, 16225 Eberswalde, Germany

<sup>4</sup> Centre of Excellence for Wood and Forestry, Public Enterprise Sachsenforst, 01796 Pirna, Germany; Rainer.Petzold@smul.sachsen.de

\* Correspondence: Stefan.Julich@tu-dresden.de

**Abstract:** Tree species, e.g., shallow vs. deep rooting tree species, have a distinct impact on hydrological properties and pore size distribution of soils. In our study, we determined the soil hydrologic properties and pore size distribution at three forest stands and one pasture as reference on soils with stagnant water conditions. All sites are located in the Wermsdorf Forest, where historical studies have demonstrated severe silvicultural problems associated with stagnant water in the soil. The studied stands represent different stages of forest management with a young 25-year-old oak (Sessile Oak (*Quercus petraea*) and Red oak (*Q. robur*)) plantation, a 170-year-old oak stand and a 95-year-old Norway Spruce (*Picea abies*) stand in second rotation. We determined the infiltration rates under saturated and near-saturated conditions with a hood-infiltrometer at the topsoil as well as the saturated hydraulic conductivity and water retention characteristic from undisturbed soil samples taken from the surface and 30 cm depth. We used the bi-modal Kosugi function to calculate the water retention characteristic and applied the normalized Young-Laplace equation to determine the pore size distribution of the soil samples. Our results show that the soils of the old stands have higher amounts of transmission pores, which lead to higher infiltration rates and conductance of water into the subsoil. Moreover, the air capacity under the old oak was highest at the surface and at 30 cm depth. There was also an observable difference between the spruce and oak regarding their contrasting root system architecture. Under the oak, higher hydraulic conductivities and air capacities were observed, which may indicate a higher and wider connected macropore system. Our results confirm other findings that higher infiltration rates due to higher abundance of macropores can be found in older forest stands. Our results also demonstrate that an adapted forest management is important, especially at sites affected by stagnant water conditions. However, more measurements are needed to expand the existing data base of soil hydraulic properties of forest soils in temperate climates.

**Keywords:** soil hydraulic properties; water retention; infiltration rates; tree species; forest management; soil structure



**Citation:** Julich, S.; Kreiselmeier, J.; Scheibler, S.; Petzold, R.; Schwärzel, K.; Feger, K.-H. Hydraulic Properties of Forest Soils with Stagnic Conditions. *Forests* **2021**, *12*, 1113. <https://doi.org/10.3390/f12081113>

Received: 8 July 2021

Accepted: 16 August 2021

Published: 20 August 2021

**Publisher's Note:** MDPI stays neutral with regard to jurisdictional claims in published maps and institutional affiliations.



**Copyright:** © 2021 by the authors. Licensee MDPI, Basel, Switzerland. This article is an open access article distributed under the terms and conditions of the Creative Commons Attribution (CC BY) license (<https://creativecommons.org/licenses/by/4.0/>).

## 1. Introduction

Several hydrologic ecosystem services provided by forests such as flow regulation and water provision are related to the ability of soils to store and transmit water [1–3]. Water storage and transmission properties of soils are quantified by the water retention and hydraulic conductivity function (hereinafter referred to as soil hydraulic properties, SHP). Compared to other land-uses, forest soils often have a higher infiltration rate and saturated hydraulic conductivity of the topsoil [4–7]. The higher infiltration rate of forest soils is

associated with a higher abundance of macropores [8,9] and a higher connectivity of larger pores [1,4,10]. Besides macrofaunal activity, it is mainly the turnover and decay of roots that control the size and stability of pores in the soil. For cropland soils, Bodner et al. [11] found that coarse roots increase macroporosity while fine root systems induce a higher micropore volume. In stagnic soils with low biotic activity, coarse roots have a strong control on preferential infiltration [9]. This has implications for runoff generation processes and therefore on the role of forests in the hydrological cycle at the landscape scale [12–15].

SHP are influenced by the characteristics of the respective soil as well as by land use and land management over space and time [16–19] (among others). SHP of soils are determined by measuring hydraulic conductivity and water retention characteristics; the latter are used to derive pore size distribution [20–22]. In contrast to forest ecosystems, the impact of land management and agricultural management on SHP has been widely studied [18,23]. There is clear evidence that agricultural practices such as tillage, fertilization, and fallowing affect SHP [16,18,21,22] (among others). In contrast to agricultural sites, only few studies have characterized SHP of soils from forests in temperate climates. Many studies have focused mainly on the effect of forest management practices such as thinning as well as skidding and forwarding of wood on SHP [24–26]. Only few studies compared the impact of tree species and age and structure on SHP. Wahren et al. [14] compared afforestation of different ages and a near-natural forest and observed significant differences in SHP between the stands. Hayashi et al. [27] found higher median pore radius and width of distribution in undisturbed forest soils compared to disturbed soils due to development of secondary soil pores. For different forest types in a tropical monsoon region, differences in available water capacity and volume of coarse pores between deciduous and evergreen trees were reported [28]. Higher infiltration rates under Scotts Pine (*Pinus sylvestris*) versus under Sycamore (*Acer pseudoplatanus*) and pasture were measured by Chandler et al. [6]. Other studies demonstrated that afforestation leads to increased infiltration rates and saturated hydraulic conductivity in the topsoil [3,29]. Archer et al. [1] found that, for temperate zone forests, infiltration rates, abundance, and connectivity of macropores increased with stand age.

In this study, we determined hydraulic properties and pore size distribution of soils with stagnic conditions under forests differing in type and age in the Wermsdorf Forest (Saxony). This site is known to be highly problematic concerning their forest management over an extended period [30,31]. The Wermsdorf area played an important role in the recognition and silvicultural-ecological assessment of stagnic soils (“gleiartige Böden”) in contrast to groundwater-affected soils [30]. From their comprehensive field studies, Krauss et al. [32] concluded that the growth problems in the second and subsequent generations of spruce monocultures was mostly attributable to a marked change in the soil physical conditions, i.e., the loss of coarse pores that had been formed by the previous oak stands. We selected three forest sites with different tree species and stand age and a meadow as a reference site. Here, in situ infiltration rate at saturation and near saturation at the soil surface and SHP were determined. The objective of our study was to expand the knowledge on SHP of forest soils of the temperate climate zones. We hypothesize that there are differences in SHP and pore size distributions within the different forest stands as well as between the forest and meadow sites.

## 2. Materials and Methods

### 2.1. Site Description and Historical Silvicultural-Ecological Background

We selected four sites in the Wermsdorf Forest (Wermsdorfer Wald), a state-owned forest covering an area of about 5100 ha in the lowlands of northwestern Saxony (northeastern Germany). The area (approx. 200 m above sea level) has a long-term annual air-temperature of 8.5 °C and a mean annual precipitation of 610 mm. All sites were within the forest district, Collm, with a total area of 1345 ha. The terrain was flat to slightly undulating. Three sites were supposed to represent a chronosequence of forest conversion from a third-generation spruce stand (SPR95), over a 25-year-old oak afforestation (OAK25), to

an old mixed deciduous stand (OAK170). A fourth site, used as a reference, was a meadow (MEA). The soil of the selected sites derived from periglacial reworked loess loam underlain by glacial till. Texture was comparable at all sites with silt being the dominating fraction (Table 1). The soil type of the different stands was a Pseudogley (German classification, or a Haplic Stagnosol according to World Reference Base). An overview of the sites is presented in Figure 1. Below, we list the sites and their characteristics:

SPR95: This site was a pure stand of Norway spruce (*Picea abies*) in its second generation with an approximate age of 95 years. Due to the dense stagnic horizon of the Stagnosol trees at this site, trees only formed shallow roots that lead to frequent windthrow.

OAK25: This site was directly adjacent to MEA. It had been afforested with oak about 25 years prior to this study and with individual trees of European Beech (*Fagus sylvatica*), Silver Birch (*Betula pendula*), and European Aspen (*Populus tremula*).

OAK170: This site represented the “target state” of the local forest conversion program. The area of this site was formerly used for hunting and was therefore not subject to extensive forest transformation in the past. Sessile oak (*Quercus petraea*) and European oak (*Quercus robur*) were the most abundant tree species. The age of the oldest trees was about 170 years. Further species found were Maple (*Acer platanoides*) and Hornbeam (*Carpinus betulus*). European and Sessile oak with hornbeam are the dominant species in the potential natural forest association [32].

MEA: The unmanaged meadow used to be a feeding place for game 30 years prior to our study. It was directly adjacent to the OAK25 site. A ploughing horizon was still clearly visible down to 20–25 cm depth. Signs of wild boar activity were visible on the soil surface in certain areas, which were avoided as sites for the experiments.

**Table 1.** Basic soil properties of the four sites. Analysis for texture and C and N were performed using bulk samples per horizon. Bulk density was determined by 100 cm<sup>3</sup> rings in 5 repetitions. Here, arithmetic mean and standard deviation (in brackets) are presented. Stone content was negligible in all analyzed horizons. Description of the horizons are according to WRB. n.d., not determined.

Site-Horizon	Depth (cm)	Sand/Silt/Clay (Mass-%)	Bulk Density (g cm <sup>-3</sup> ) (n = 5)	C (Mass%)	N (Mass%)
MEA-Ah	0–25	13/70/17	1.19 (0.09)	1.98	0.14
MEA-Bg	25–45	13/73/14	1.53 (0.09)	0.16	0.03
MEA-2Bg	45–76	45/38/17	1.52 (0.04)	0.12	0.02
OAK25-Ah	0–18	12/68/20	1.25 (0.01)	2.33	0.17
OAK25-AhBg	18–32	13/67/20	1.48 (0.07)	1.14	0.08
OAK25-Bg	32–50	43/35/21	1.75 (0.02)	0.18	0.02
OAK25-Btg	50–90	42/24 /35	1.70 (0.06)	0.08	0.02
OAK170-Oa/Ah	0–10	12/66/22	0.87 (0.15)	11.5	0.67
OAK170-Bw	10–31	7/78/15	1.48 (0.11)	0.77	0.05
OAK170-Bg	31–60	6/72/22	1.48 (0.03)	0.47	0.05
OAK170-Btg	60–90	42/20/38	1.75 (0.06)	0.13	0.02
SPR95-Oa/Ah	0–3	18/64/19	n.d.	10.6	0.51
SPR95-EBg	3–38	25/65/10	1.53 (0.07)	0.61	0.04
SPR95-Bg	38–90	44/31/25	1.57 (0.07)	0.17	0.03

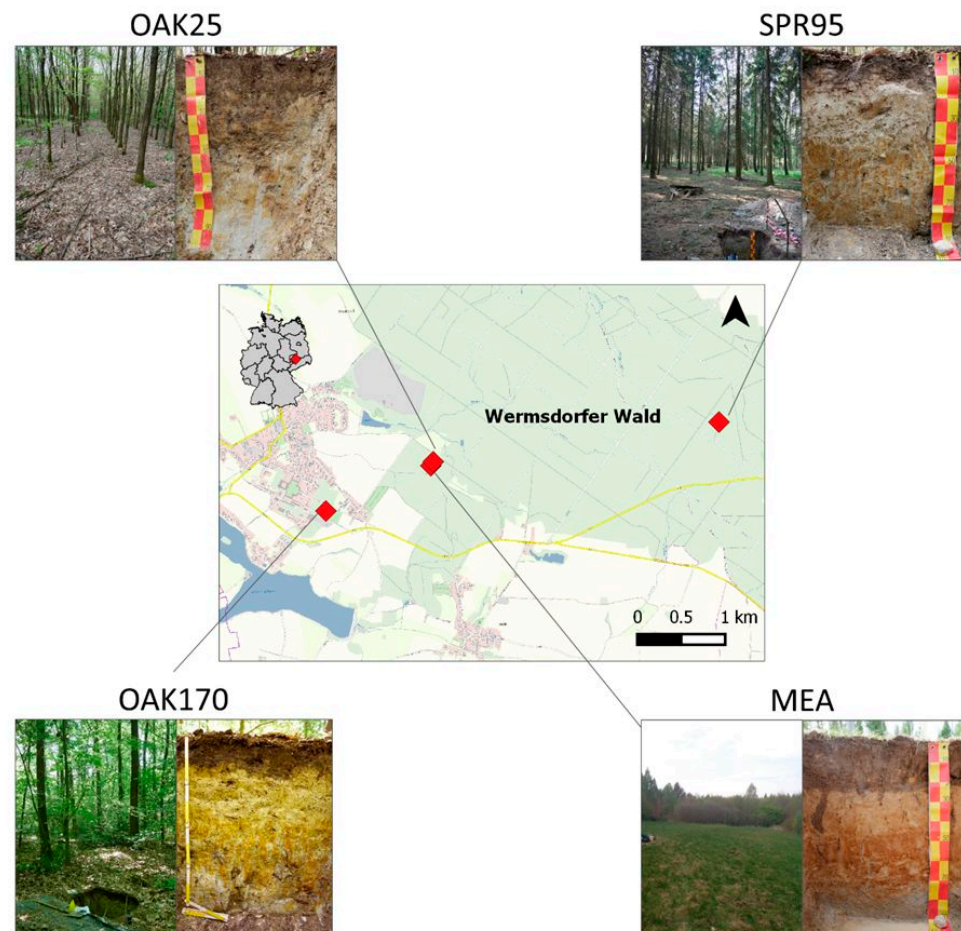


**Figure 1.** Overview over the site locations in the Wermsdorf Forest with photos of the surroundings and the respective soil profile. SPR95 = 95-year-old spruce stand in second generation; OAK25 = 25-year-old oak afforestation; OAK170 = old mixed deciduous stand with oaks up to 170 years old; MEA = meadow used as reference.

## 2.2. Infiltration Measurements

For the determination of field hydraulic conductivity at saturated and near-saturated conditions, we conducted a set of seven infiltration measurements with a hood infiltrometer (hood size 12.4 cm radius, infiltration area = 483 cm<sup>2</sup>) (HI, in accordance with Schwärzel and Punzel [33]) at each site at the soil surface. The measurements were performed at the surface after carefully removing the organic layer in advance on the forested sites and the sod on MEA. Planned subsoil measurements with the HI at 30 cm depth failed on most sites except for MEA due to the low conductivity in the stagnant horizon of the soil profiles. Nominal pressure heads were 0 and −1 cm. Water was left to infiltrate until steady state was reached. Analysis of the infiltration rates was performed following the linear interpolation procedures outlined in Reynolds and Elrick [34] and Ankeny et al. [35].

## 2.3. Water Retention and Pore Size Distribution

For a general characterization of the soil properties at each site, descriptive soil pits were established. To determine texture, bulk density, and content of organic material, bulk samples and soil core rings (100 cm<sup>3</sup> in 5 repetitions) were retrieved in each diagnostic horizon. Soil texture was obtained from the combined sieving and sedimentation analysis. Total C and N contents of grounded samples were determined after dry combustion with a CN analyzer (Vario EL III Elementar GmbH, Hanau, Germany). The soils contained no inorganic C, thus soil organic C (SOC) equaled total C. At the center of the infiltration experiments, undisturbed soil cores of 250 cm<sup>3</sup> (height of the cylinders was 5 cm) were



retrieved from the surface of the first mineral horizon. The samples were obtained after 24 h from the infiltration measurements, giving the soil time to drain and to ensure a smooth sampling. Afterward, samples from the subsoil at 30 cm depth were obtained. The retrieved soil cores were used for the determination of the water retention characteristic (WRC) and saturated hydraulic conductivity (Ks). The additional determination of Ks in the lab was conducted for comparison of the field saturated conductivity in accordance with Reynolds et al. [36] and Bagarello et al. [37], who found that the combination of methods delivers more reliable results for structured soils. In the lab, samples were fitted with a porous plate and placed in a trough filled with tap water for saturation. Water levels were gradually raised to reduce the risk of air entrapment. Upon saturation, Ks was determined with the falling head method using the KSAT<sup>®</sup> device (METER Environment, Munich, Germany). Subsequently, saturated soil cores were assembled with the HYPROP<sup>®</sup> system (METER Environment, Munich, Germany) to determine the WRC through a transient evaporation experiment (measurement range pF0 to pF3). With the HYPROP-Fit software (METER, 2019, Soil Physics UMS GmbH, Munich, Germany), we fitted the bimodal version of the Kosugi-WRC [21,38] from the measurements of each individual soil core. Similar to Kreiselmeyer et al. [21], we calculated the pore size distribution (PSD) with the normalized version of the Young-Laplace equation. We determined the pore volume according to Kreiselmeyer et al. [21] for the different pore size classes as defined by Greenland [39] from the area under the curve of the bimodal PSD, resulting in fissures ( $\varnothing > 500 \mu\text{m}$ ), transmission ( $\varnothing 50\text{--}500 \mu\text{m}$ ), and storage ( $\varnothing 1.49\text{--}50 \mu\text{m}$ ). We assigned all pores with pore sizes corresponding to a pressure head that was outside the measurement range of the HYPROP system to the class fine pores ( $\varnothing < 1.49 \mu\text{m}$ ).

#### 2.4. Statistical Analysis

For the statistical analysis, R 3.6.2 (R Development Core Team, 2017, Brussels, Belgium) was used. All conductivity values were log-normal transformed for analysis and determination of the standard deviation. For the quantities of hydraulic conductivity, bulk density (BD), and the respective pore size classes, one-side analysis of variance using the emmeans package in R [40] was performed to identify the influence of site properties versus forest management. The significance level was  $p < 0.05$  for all statistical tests.

### 3. Results

#### 3.1. Basic Soil Properties

Basic soil properties that were determined from the descriptive soil pits are summarized in Table 1. The texture was similar in all analyzed soil profiles, with silt dominating in the upper horizons and an increasing sand content in the lower horizons. At all sites, the stone content was negligible. Bulk density of the first horizons was, in order, OAK25 ( $1.25 \text{ g cm}^3$ ) > MEA ( $1.19 \text{ g cm}^3$ ) > OAK170 ( $0.87 \text{ g cm}^3$ ) > SPR95 ( $0.58 \text{ g cm}^3$ ). Bulk Density determined with  $100 \text{ cm}^3$  cylinders for the respective diagnostic horizons increased at all sites, with maximum values of  $1.75 \text{ g cm}^3$  at the oak sites at a depth between 50 and 90 cm. Carbon and nitrogen content of the first horizon followed the order: OAK170 (11.5% C and 0.67% N) > SPR95 (10.6% C and 0.51% N) > OAK25 (2.3% C and 0.17% N) > MEA (2.0% C and 0.14% N). However, the separation between the organic layer and the top mineral soil was difficult. Therefore, the samples from the uppermost, thin mineral soil horizons partly covered Oa-material (Oa/Ah). Carbon and nitrogen content decreased significantly with the lower horizons, keeping the same order as in the first horizons.

#### 3.2. Infiltration Experiments

The hydraulic conductivity at the surface under saturated (Kfs) and near-saturated (Kfns) conditions was determined with the hood infiltrometer (Figure 2). The median of Kfs was 3.04, 2.79, 2.67,  $2.46 \text{ cm day}^{-1}$  for OAK170, MEA, SPR95, and OAK25, respectively. A significant difference was only observable between OAK170 and OAK25 (at  $p < 0.05$ ).

The standard deviation of Kfs for the sites ranged between 0.41 cm day<sup>-1</sup> for Oak25 and 0.15 cm day<sup>-1</sup> for SPR95.

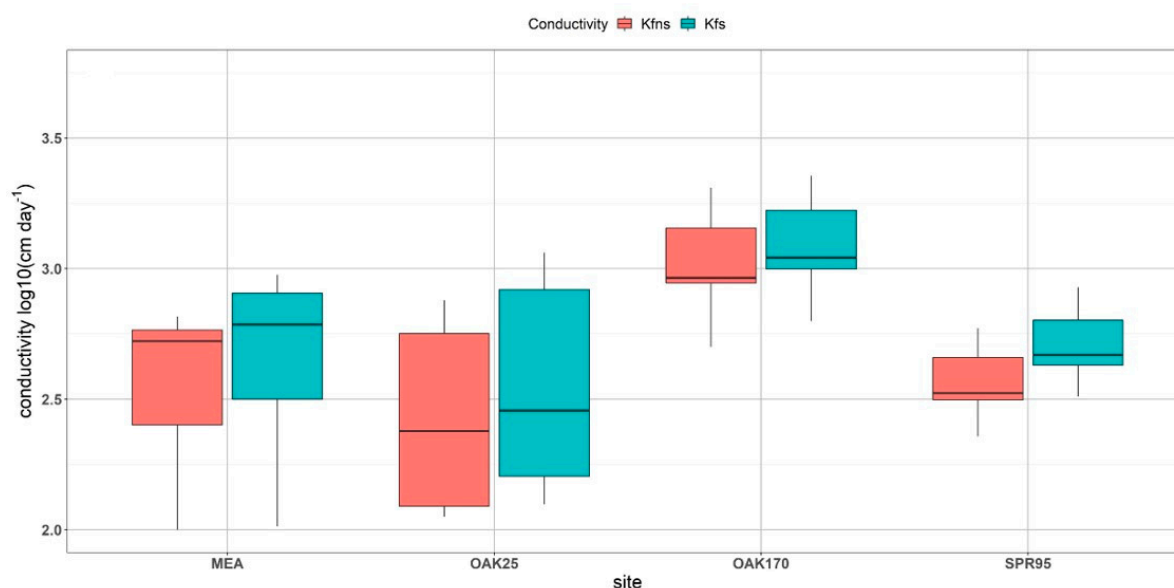


**Figure 2.** Field conductivity (log10 transformed in cm day<sup>-1</sup>) under saturated (Kfs) and near-saturated ( $|h| = -1$  cm) (Kfns) at the four sites.

The median of Kfns ( $|h| = -1$  cm) was 2.96 cm day<sup>-1</sup> for OAK170, 2.72 cm day<sup>-1</sup> for MEA, 2.52 cm day<sup>-1</sup> for SPR95, and 2.38 cm day<sup>-1</sup> for OAK25. Statistical analysis revealed a significant difference between OAK170 and OAK 25 ( $p < 0.01$ ) and significant differences ( $p < 0.05$ ) between MEA and OAK170 as well as between SPR95 and OAK170. The standard deviation ranged from 0.37 cm day<sup>-1</sup> for OAK25 to 0.15 cm day<sup>-1</sup> for SPR 95.

### 3.3. Properties Derived from Undisturbed Soil Sampling

The median of the bulk density from samples obtained from the surface (Figure 3a) was 1.35 g cm<sup>-3</sup> for SPR95, 1.19 g cm<sup>-3</sup> for MEA, 1.17 g cm<sup>-3</sup> for OAK25, and 1.0 g cm<sup>-3</sup> for OAK170. As can be seen from the figure (Figure 3a), there was no significant difference between the sites. The standard deviations range from 0.23 g cm<sup>-3</sup> for SPR95 to 0.07 g cm<sup>-3</sup> for OAK25.

Bulk density from the samples at 30 cm depth showed a highly significant difference between MEA and OAK170 and between OAK170 and OAK25 ( $p < 0.001$ ) and a significant difference between MEA and SPR95 and OAK25 and SPR95 ( $p < 0.05$ ). The median of bulk density followed the order OAK25 (1.6 g cm<sup>-3</sup>) = MEA (1.6 g cm<sup>-3</sup>) > SPR95 (1.43 g cm<sup>-3</sup>) > OAK170 (g cm<sup>-3</sup>). The standard deviation of the bulk density was OAK170 (0.09 g cm<sup>-3</sup>) > SPR95 (0.07 g cm<sup>-3</sup>) > MEA (0.05 g cm<sup>-3</sup>)  $\approx$  OAK25 (0.04 g cm<sup>-3</sup>), indicating a low variation at all sides.

The median of Ks (Figure 3b) from the 250 cm<sup>3</sup> cores obtained at the surface and derived with the falling head method was 3.45 cm day<sup>-1</sup> for OAK170, 3.3 cm day<sup>-1</sup> for OAK25, 2.43 cm day<sup>-1</sup> for SPR95, and for MEA 2.23 cm day<sup>-1</sup>. Statistical analysis revealed no significant differences among the samples and the standard deviation of Ks ranged from 0.86 cm day<sup>-1</sup> for OAK170 to 0.34 cm day<sup>-1</sup> for OAK25.

The median of Ks from the samples obtained at 30 cm depth was 2.75 cm day<sup>-1</sup> for OAK170 and OAK25, 2.25 cm day<sup>-1</sup> for MEA and 1.63 cm day<sup>-1</sup> for SPR95. The statistical analysis yielded no significant difference between the sites. The standard deviation was between 1.93 cm day<sup>-1</sup> for OAK25 and 0.32 cm day<sup>-1</sup> for OAK170. This shows a high variation for OAK25 and MEA and a lower variation for OAK170 and SPR95.

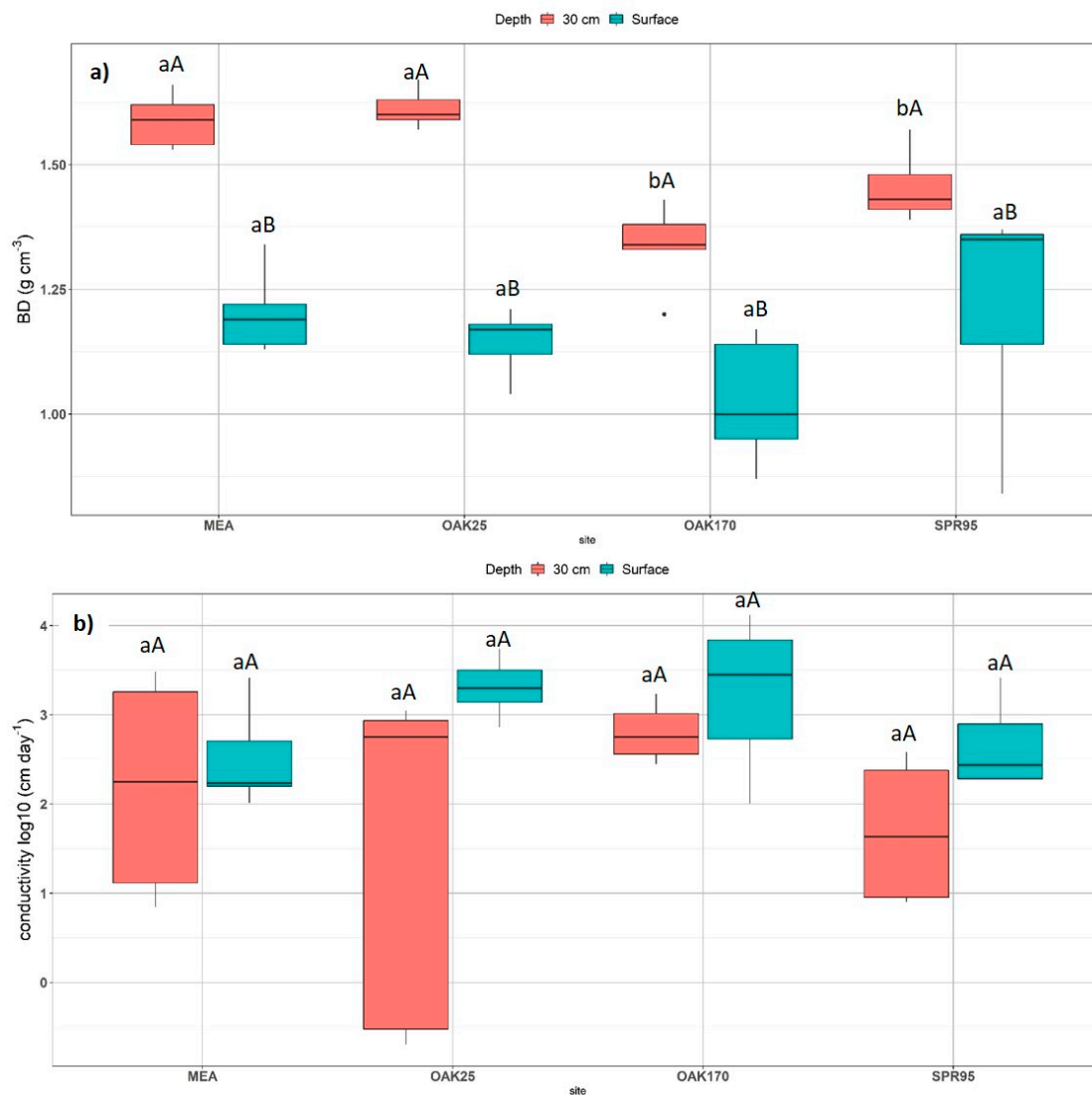


**Figure 3.** Bulk density (a) and saturated hydraulic conductivity (log<sub>10</sub>) measured in the laboratory and (b) derived from the 250 cm<sup>3</sup> cores for the four sites for surface and 30 cm depth, respectively; sample size  $n = 5$  for all sites and depths. Same lowercase letters indicate no significant differences among sites ( $p < 0.05$ ). Same uppercase letters in a column indicate no significant differences within the sites among depth ( $p < 0.05$ ).

### 3.4. Water Retention

Table 2 presents the parameters of the water retention curves for the topsoil and subsoil samples. The mean of RMSE (root mean square error) for the water retention curves and the conductivity curve are low, indicating a good fit to the observed data points. The mean  $\theta_r$  of the topsoil samples was highest for SPR95 (0.074) and lowest for MEA (0.0274) with OAK25 and OAK170 having values between SPR95 and MEA. The standard deviation is largest for OAK25 and lowest for OAK170. The standard deviation of the other sites is between OAK25 and OAK170. The  $\theta_r$  of the samples from 30 cm depth were highest for SPR95 and OAK25 (0.08) and lowest for OAK170 (0.052). Standard deviation was lowest for MEA and SPR95 and similar for OAK25 and OAK95. The  $\theta_s$  for the samples obtained from the surface were highest for MEA (0.541) and lowest for SPR95 (0.47); the other sites were in between. The standard deviation was highest for SPR95 and lowest for OAK170. The  $\theta_s$  for the samples obtained from 30 cm depth: OAK170 was the highest (0.41), and MEA and OAK25 (0.38) were the lowest, showing approximately similar values for all sites. Standard deviation was lowest in OAK25 and highest in OAK170. The other parameters

show no clear pattern between the sites, indicating the large heterogeneity between sites as well as between samples.

**Table 2.** Means of the water retention curve parameters fitted with the bimodal Kosugi model; residual ( $\theta_r$ ) and saturated ( $\theta_s$ ) water content, pressure heads at effective saturation  $Se_i(h_{mi}) = 0.5$  for both the structural ( $hm_1$ ) and textural ( $hm_2$ ) domains, their respective standard deviations of the lognormal pore radii  $\sigma_1$  and  $\sigma_2$ , and the weighting factor for the structural domain ( $w_1$ ). The weighting factor of textural domain ( $w_2$ ) can be obtained by  $1-w_1$ . Saturated hydraulic conductivity ( $K_s$ ) is presented as geometric mean of laboratory falling head measurements. Goodness of fit between observed and modeled values is expressed by the root mean square error (RMSE) for both the water retention and hydraulic conductivity characteristic. Standard deviation is presented in brackets.

		$\theta_r$	$\theta_s$	$hm_1$	$hm_2$	$rm_1$	$rm_2$	$\sigma_1$	$\sigma_2$	$w_1$	$K_s$	RMSE th	RMSE K
		$cm^3 cm^{-3}$		cm		$\mu m$			(-)		$cm day^{-1}$	$cm^3 cm^{-3}$	$Log_{10}(cm day^{-1})$
Surface	MEA	0.0274 (0.0523)	0.541 (0.0293)	708.2 (786.9)	1962.4 (1437.4)	10.5 (17.3)	1.6 (1.6)	1.02 (0.87)	1.84 (0.76)	0.66 (0.31)	2.51 (0.56)	0.0019 (0.001)	0.1257 (0.1854)
	OAK25	0.0506 (0.0704)	0.492 (0.034)	1158.2 (1558.0)	1961.0 (1681.9)	4.9 (6.5)	27.8 (60.2)	1.82 (1.35)	2.18 (1.47)	0.55 (0.29)	3.31 (0.34)	0.0016 (0.0005)	0.0815 (0.0181)
	OAK170	0.050 (0.037)	0.490 (0.019)	446.4 (278.8)	2764.0 (4223.2)	4.7 (3.3)	3.7 (3.1)	1.72 (1.05)	2.40 (1.53)	0.52 (0.31)	3.23 (0.86)	0.0017 (0.0007)	0.0679 (0.0309)
	SPR95	0.074 (0.052)	0.471 (0.080)	253.6 (243.0)	597.4 (508.8)	47.9 (92.3)	18.1 (33.8)	0.91 (0.33)	2.22 (0.82)	0.67 (0.30)	2.66 (0.5)	0.0020 (0.0010)	0.0669 (0.0330)
30 cm	MEA	0.063 (0.029)	0.378 (0.027)	2044.4 (2140.4)	1081.0 (917.6)	15.0 (31.3)	8.3 (15.2)	1.36 (0.84)	1.09 (0.72)	0.44 (0.42)	2.19 (1.20)	0.0014 (0.0005)	0.1611 (0.0630)
	OAK25	0.080 (0.062)	0.375 (0.009)	2367.8 (4276.9)	4095.4 (4133.2)	19.2 (38.3)	1.0 (1.0)	0.80 (0.64)	1.69 (0.92)	0.75 (0.23)	1.5 (1.93)	0.0021 (0.0012)	0.1154 (0.0221)
	OAK170	0.059 (0.062)	0.412 (0.031)	575.8 (416.6)	772.6 (1077.3)	11.8 (21.2)	35.4 (46.3)	1.10 (0.82)	1.93 (1.15)	0.55 (0.33)	2.80 (0.32)	0.0024 (0.0019)	0.0736 (0.0492)
	SPR95	0.080 (0.030)	0.398 (0.028)	362.4 (301.3)	504.6 (428.5)	27.0 (45.1)	8.9 (9.5)	0.83 (0.53)	1.13 (0.97)	0.58 (0.40)	1.69 (0.78)	0.0036 (0.0027)	0.1089 (0.0435)

Table 3 presents air capacity, field capacity, available water capacity, and permanent wilting points of the samples derived from the above-described water retention functions. For the samples taken at the surface, the old forest stands (OAK170 and SPR95) had a significantly higher air capacity than MEA and OAK25. For field capacity and available water capacity, MEA had significantly higher values than the other sites. For the water content at the permanent wilting point, no significant difference was observable between all sites. At 30 cm depth there were no significant differences between sites except for air capacity, which was significantly higher for OAK170.

**Table 3.** Volume fractions for air capacity (AC) ( $\theta$  between  $pF_0$  and  $pF_{1.8}$ ), field capacity (FC) ( $\theta$  at  $pF_{1.8}$ ), available water capacity (AWC) ( $\theta$  between  $pF_{1.8}$  and  $pF_{4.2}$ ), and permanent wilting point (PWP) ( $\theta$  at  $pF_{4.2}$ ) under meadow (MEA), young oak (OAK25), old oak (OAK170), and spruce (SPR95). Same lowercase letters are not significantly different at  $p < 0.05$  (LSD) among sites.

Depth	Site	AC (Vol.-%)		FC (Vol.-%)		AWC (Vol.-%)		PWP (Vol.-%)	
		Mean	Sd	Mean	Sd	Mean	Sd	Mean	Sd
Surface	MEA	a2.7	1.2	a51.4	2.4	a40.8	2.8	a10.6	2.0
	OAK25	ab6.0	2.2	b42.6	5.4	b28.8	4.0	a13.8	1.7
	OAK170	b8.1	2.4	b40.3	3.7	b29.1	2.8	a11.2	2.1
	SPR95	b7.0	2.8	b39.9	5.2	b29.6	4.1	a10.3	2.6
30 cm	MEA	a1.5	0.9	a36.1	2.2	a25.5	2.2	a10.9	0.9
	OAK25	a1.3	0.6	a36.3	1.1	a23.1	7.3	a13.1	7.4
	OAK170	b5.7	1.7	a35.2	1.7	a26.5	4.9	a8.7	5.0
	SPR95	a3.0	1.9	a36.8	4.7	a27.7	3.8	a9.1	1.1



### 3.5. Pore Size Distribution

Figure 4 presents the pore volume fraction of samples retrieved from the surface and at 30 cm depth for fissures ( $\varnothing > 500 \mu\text{m}$ ), transmission ( $\varnothing 50\text{--}500 \mu\text{m}$ ), storage ( $\varnothing 1.49\text{--}50 \mu\text{m}$ ), and fine pores ( $\varnothing < 1.49 \mu\text{m}$ ) [39] obtained from the area under PSD curves considering  $\Phi$ . For the surface as well as the subsoil samples, the storage and fine fractions of the pores had the largest volume. Fissures had the lowest volume of pore size distribution. Among the surface samples, there was a significant difference in the amount of fissures between the MEA and OAK25/OAK170. For the transmission pores, a significant difference between MEA and the two old forest stands was observable. For the domain of the storage pores, no difference between the sites was observed. In the domain of the fine pores only, SPR95 was significantly different from the other site, however since this domain is outside the measured range of the water retention, that difference may be due to the extrapolation.

For the samples taken from 30 cm depth, differences among the sites for the different pore size classes were more pronounced. For fissures and transmission pores, OAK170 was significantly higher than the other sites. For storage pores, the old forest stands were significantly different from MEA and OAK25. For the class of fine pores, no significant difference among the sites was observed.

## 4. Discussion

### *Soil Hydraulic Properties of Forest Soils with Stagnant Conditions*

Our measurements exhibited similar differences in the SHP between the different sites as in comparable studies [1,7]. Regarding the basic soil properties of the topsoil bulk density and organic matter content found in the meadow (MEA) and the young oak afforestation (OAK25), they are similar to values of sites with comparable characteristics [1,14]. They are also similar to agricultural sites with reduced human influence such as no tillage practices [21]. At the meadow site, a ploughing horizon of 25 cm in thickness was still visible 30 years after conversion. The increased bulk densities and lower organic carbon contents in the topsoil of the young oak afforestation may be because for oak planting, the young trees are normally taken from the nursery where taproots are cut before transplantation. Because of higher input in biomass and lower human disturbance the organic matter content was higher and bulk density was lower at the older forest sites and comparable with other sites with similar tree age [1,4,14,41]. The basic properties of the subsoil are in the reported range of comparable sites [1,14,41]. Texture, bulk density, and organic matter content influence the water retention characteristic and pore size distribution of soils [19]. The water retention characteristics (Table 3) for the topsoil and subsoil show that the old oak stand (OAK170) has a higher air capacity. The higher aeration has positive effects on the growth of the rooting system in soils with waterlogging conditions. The OAK170 site is characterized by a continuous stocking with oak and other deciduous tree species at least since medieval times. This indicates that a long-term natural root development of trees originating from natural regeneration via seedlings was possible. Therefore, a deep-reaching rooting and corresponding (macro-) pore system was continuously existent. Archer et al. [1] also found a higher abundance of macropores under old forest stands (>200 years). Our findings support the conclusions based on the root excavations of Wermsdorf by Krauss et al. [33], who found a deep developed root system under oak and a shallow root network under spruce.

The above-stated findings are seen together with the pore size distributions. The old oak stand in the topsoil contains a higher portion of fissures ( $\varnothing > 500 \mu\text{m}$ ) and transmission pores ( $\varnothing 50\text{--}500 \mu\text{m}$ ), whereas OAK25 and meadow contain more storage pores ( $\varnothing 1.49\text{--}50 \mu\text{m}$ ). This is related to the development of the rooting system and the corresponding formation of macropores. Several studies show that the development and formation of macropores and associated preferential flow paths are linked with living roots as well as root channels from decaying roots and drying-wetting processes, which may be more intense under trees [8–10,42]. These pores can be stable for a longer period of time [43]. The differences in pore size distributions are more pronounced in the subsoil.

Here, the old oak stand has significantly higher portions of fissures and transmission pores than the other sites, which can be associated with architecture and average length of the rooting system [44–46]. The significantly higher amount of storage pores at the old forest stands can be related to the higher amount of organic material.

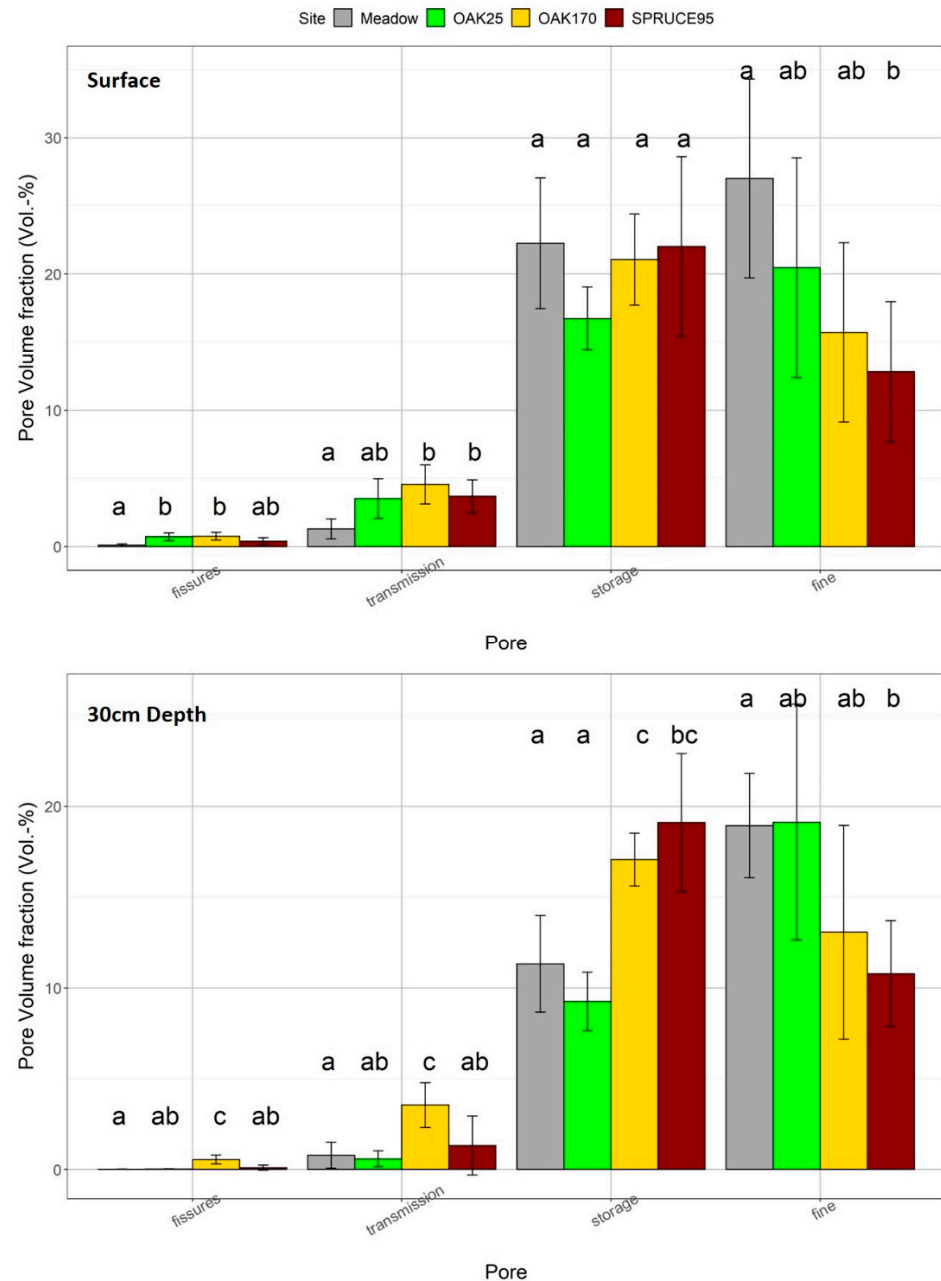


**Figure 4.** Volume fraction of different pore size classes for the samples from the surface (upper plot) and samples from 30 cm depth (lower plot) obtained from the area under bimodal pore size distribution. Classes were fissures (diameter  $\varnothing > 500 \mu\text{m}$ ), transmission ( $\varnothing 50\text{--}500 \mu\text{m}$ ), storage ( $\varnothing 1.5\text{--}50 \mu\text{m}$ ), and fine pores ( $\varnothing < 1.5 \mu\text{m}$ ). Fissures, transmission, and storage pores are derived from the measured part of the water retention curve, and the fine pores are determined from the extrapolated part of the water retention curve. Same lowercase letters over the bars are not significantly different at  $p < 0.05$  among the pore size classes.

Linked with the pore size distribution is the hydraulic conductivity of soils [19]. Higher amounts of macropores and higher connectivity of such pores favor increased infiltration rates [1,4,6,10,14,41,42]. This is confirmed by our measurements. The Kfs was

highest at the forest stands with the oldest age, especially for OAK170. The median of Kfs was highest for OAK170, followed by SPR95. These results are consistent with other studies from temperate forests of different ages. Wahren et al. [7] and Archer et al. [1] found similar infiltration rates for log10 Kfs around 3 cm day<sup>-1</sup>. They also found higher Kfs in older forest stands compared to stands of younger age. Furthermore, Archer et al. [4] found higher values for Kfs in older broadleaved stands than in surrounding grasslands. The highest differences between the four sites can be observed for the field hydraulic conductivity at near-saturation Kfns ( $h = -1$  cm). The differences between Kfs and Kfns indicate how many large pores-like cracks and fissures dominate the infiltration process at saturation. For OAK170, Kfns is higher than Kfs for the other sites, which may indicate the effect of the more developed and deeper rooting network associated with a network of larger pores that conducts more water into deeper zones of the soil. The high Kfs and Kfns, together with the highest amount of transmission pores, at the surface and at 30 cm depth support this finding. The higher Ks values of the soil cores of the forest stands can be associated with the higher amount of larger pores. Other studies found increasing Ks with an increasing amount of larger pores and organic content and decreasing bulk density [1,4,8,14,21,41,42]. The high variability in Ks measurements can be linked with the measurement method in which biopores such as root channels can dominate the flow processes in the relatively short soil cores (height = 5 cm) [21,36]. This may explain the differences in infiltration rates between the old oak and spruce stands. Spruce develops a shallow rooting system that can be impeded by waterlogging conditions in the soil [9,47]. Oaks form a deeper rooting system with the ability to penetrate dense horizons and those affected by stagnant water [33,45,46].

## 5. Conclusions

Our results confirm those of other studies that found higher amounts of macropores and higher infiltration rates under old forest stands. We can also show the influence of stagnant water conditions on the development of the rooting system and its consequences on SHP. The soil under the old oak stand exhibited higher amounts of coarse transmission pores, which favor aeration, higher infiltration, and conductance of water into deeper soil zones compared to the other sites. Our data support the conclusions from old root excavation studies that addressed the change of soil physical conditions at spruce afforestations on stagnosol sites. Furthermore, our experimental findings and calculations of pore size distribution and functionalities support their claim for soil structure restoration by planting of oak, thus benefiting from the rooting activity of that tree species natural to the site. Moreover, under oak, higher infiltration capacities due to a higher and wider connected macropore system could be observed. At a larger spatial scale, this not only has implications on hydrologic ecosystem services such as water retention but also on the water economy of trees themselves and therefore on the vulnerability of the forest stands to drought.

Our results demonstrate the importance of site-adapted forest management, especially in areas with soils with a problematic structure, which thus may be affected by stagnant water. Such sites appear to be vulnerable to periods of extended drought. Under these conditions, deep rooting trees such as oak appear to be more adapted and able to form resilient forest stands than shallow rooting trees such as spruce. However, the changes in soil structure and SHP due to a change of tree species is a long process that can take several decades. In recent decades, the conversion of spruce afforestations in lowland areas in Saxony was a main aim of practical forestry. The transformation process will definitely be concluded as a reaction to recent climate-induced dieback of spruce (associated with bark beetle infestation). Nevertheless, our findings demonstrate the eminent potential of the applied methodology. Therefore, combined investigations of the soil's physical status with the associated soil hydraulic properties and the growth reactions of different tree species and their admixtures will gain increasing importance. This also includes the effects of contrasting vertical and horizontal rooting patterns.

**Author Contributions:** J.K., K.-H.F., K.S. and S.J. conceived the experimental approach. J.K. conducted the experiments in the field, supported by R.P. and S.S. S.J. wrote the paper as lead author. J.K., K.-H.F., K.S., R.P. and S.J. contributed equally to the discussion of the results and commented on the manuscript. All authors have read and agreed to the published version of the manuscript.

**Funding:** The research was funded by the German Research Foundation (DFG) [grant numbers SCHW 1448/6-1 and FE 504/11-1].

**Data Availability Statement:** Data of the measurements can be provided by the author upon request.

**Acknowledgments:** We thank Sachsenforst, Wermsdorf office for assistance in site selection. We are indebted to G. Ciesielski and M. Unger, who helped with laboratory measurements.

**Conflicts of Interest:** The authors declare no conflict of interest.

## References

1. Archer, N.A.L.; Otten, W.; Schmidt, S.; Bengough, G.; Shah, N.; Bonell, M. Rainfall infiltration and soil hydrological characteristics below ancient forest, planted forest and grassland in a temperate northern climate. *Ecohydrology* **2015**, *9*, 585–600. [\[CrossRef\]](#)
2. Bens, O.; Wahl, N.A.; Fischer, H.; Hüttel, R.F. Water infiltration and hydraulic conductivity in sandy cambisols: Impacts of forest transformation on soil hydrological properties. *Eur. J. For. Res.* **2006**, *126*, 101–109. [\[CrossRef\]](#)
3. Bonnesoeur, V.; Locatelli, B.; Guariguata, M.R.; Ochoa-Tocachi, B.; Vanacker, V.; Mao, Z.; Stokes, A.; Mathez-Stiefel, S.-L. Impacts of forests and forestation on hydrological services in the Andes: A systematic review. *For. Ecol. Manag.* **2019**, *433*, 569–584. [\[CrossRef\]](#)
4. Archer, N.; Bonell, M.; Coles, N.; MacDonald, A.; Auton, C.; Stevenson, R. Soil characteristics and landcover relationships on soil hydraulic conductivity at a hillslope scale: A view towards local flood management. *J. Hydrol.* **2013**, *497*, 208–222. [\[CrossRef\]](#)
5. Price, K.; Jackson, C.R.; Parker, A.J. Variation of surficial soil hydraulic properties across land uses in the southern Blue Ridge Mountains, North Carolina, USA. *J. Hydrol.* **2010**, *383*, 256–268. [\[CrossRef\]](#)
6. Chandler, K.; Stevens, C.; Binley, A.; Keith, A. Influence of tree species and forest land use on soil hydraulic conductivity and implications for surface runoff generation. *Geoderma* **2018**, *310*, 120–127. [\[CrossRef\]](#)
7. Wahren, A.; Feger, K.-H.; Schwärzel, K.; Münch, A. Land-use effects on flood generation—considering soil hydraulic measurements in modelling. In Proceedings of the Advances in Geosciences, Göttingen, Germany, 12 August 2009; Volume 21, pp. 99–107.
8. Beven, K.; Germann, P. Macropores and water flow in soils revisited. *Water Resour. Res.* **2013**, *49*, 3071–3092. [\[CrossRef\]](#)
9. Lange, B.; Lüscher, P.; Germann, P.F. Significance of tree roots for preferential infiltration in stagnic soils. *Hydrol. Earth Syst. Sci.* **2009**, *13*, 1809–1821. [\[CrossRef\]](#)
10. Alaoui, A.; Caduff, U.; Gerke, H.H.; Weingartner, R. Preferential Flow Effects on Infiltration and Runoff in Grassland and Forest Soils. *Vadose Zone J.* **2011**, *10*, 367–377. [\[CrossRef\]](#)
11. Bodner, G.; Leitner, D.; Kaul, H.-P. Coarse and fine root plants affect pore size distributions differently. *Plant Soil* **2014**, *380*, 133–151. [\[CrossRef\]](#) [\[PubMed\]](#)
12. Bosch, J.; Hewlett, J. A review of catchment experiments to determine the effect of vegetation changes on water yield and evapotranspiration. *J. Hydrol.* **1982**, *55*, 3–23. [\[CrossRef\]](#)
13. Elsenbeer, H. Hydrologic flowpaths in tropical rainforest soils—A review. *Hydrol. Process.* **2001**, *15*, 1751–1759. [\[CrossRef\]](#)
14. Wahren, A.; Schwärzel, K.; Feger, K.-H. Potentials and limitations of natural flood retention by forested land in headwater catchments: Evidence from experimental and model studies. *J. Flood Risk Manag.* **2012**, *5*, 321–335. [\[CrossRef\]](#)
15. Pilaš, I.; Feger, K.-H.; Vilhar, U.; Wahren, A. Multidimensionality of Scales and Approaches for Forest–Water Interactions. In *Forest Management and the Water Cycle: An Ecosystem-Based Approach*; Ecological Studies; Bredemeier, M., Cohen, S., Godbold, D.L., Lode, E., Pichler, V., Schleppi, P., Eds.; Springer: Dordrecht, The Netherlands, 2011; pp. 351–380. ISBN 978-90-481-9834-4.
16. Chandrasekhar, P.; Kreiselmeier, J.; Schwen, A.; Weninger, T.; Julich, S.; Feger, K.-H.; Schwärzel, K. Why We Should Include Soil Structural Dynamics of Agricultural Soils in Hydrological Models. *Water* **2018**, *10*, 1862. [\[CrossRef\]](#)
17. Robinson, D.A.; Hopmans, J.; Filipović, V.; Van Der Ploeg, M.; Lebron, I.; Jones, S.B.; Reinsch, S.; Jarvis, N.; Tuller, M. Global environmental changes impact soil hydraulic functions through biophysical feedbacks. *Glob. Chang. Biol.* **2019**, *25*, 1895–1904. [\[CrossRef\]](#)
18. Schwärzel, K.; Carrick, S.; Wahren, A.; Feger, K.-H.; Bodner, G.; Buchan, G. Soil Hydraulic Properties of Recently Tilled Soil under Cropping Rotation Compared with Two-Year Pasture. *Vadose Zone J.* **2011**, *10*, 354–366. [\[CrossRef\]](#)
19. Vereecken, H.; Huisman, J.A.; Hendricks-Franssen, H.-J.; Brüggemann, N.; Bogen, H.; Kollet, S.; Javaux, M.; Van Der Kruk, J.; Vanderborght, J. Soil hydrology: Recent methodological advances, challenges, and perspectives. *Water Resour. Res.* **2015**, *51*, 2616–2633. [\[CrossRef\]](#)
20. Assouline, S.; Or, D. Conceptual and Parametric Representation of Soil Hydraulic Properties: A Review. *Vadose Zone J.* **2013**, *12*. [\[CrossRef\]](#)
21. Kreiselmeier, J.; Chandrasekhar, P.; Weninger, T.; Schwen, A.; Julich, S.; Feger, K.-H.; Schwärzel, K. Quantification of soil pore dynamics during a winter wheat cropping cycle under different tillage regimes. *Soil Tillage Res.* **2019**, *192*, 222–232. [\[CrossRef\]](#)

22. Weninger, T.; Bodner, G.; Kreiselmeier, J.; Chandrasekhar, P.; Julich, S.; Feger, K.-H.; Schwärzel, K.; Schwen, A. Combination of Measurement Methods for a Wide-Range Description of Hydraulic Soil Properties. *Water* **2018**, *10*, 1021. [\[CrossRef\]](#)
23. Yu, M.; Zhang, L.; Xu, X.; Feger, K.-H.; Wang, Y.; Liu, W.; Schwärzel, K. Impact of land-use changes on soil hydraulic properties of Calcaric Regosols on the Loess Plateau, NW China. *J. Plant Nutr. Soil Sci.* **2015**, *178*, 486–498. [\[CrossRef\]](#)
24. Cambi, M.; Certini, G.; Neri, F.; Marchi, E. The impact of heavy traffic on forest soils: A review. *For. Ecol. Manag.* **2015**, *338*, 124–138. [\[CrossRef\]](#)
25. Di Prima, S.; Bagarello, V.; Angulo-Jaramillo, R.; Bautista, I.; Cerdà, A.; del Campo, A.; González-Sanchis, M.; Iovino, M.; Lassabatere, L.; Maetzke, F. Impacts of thinning of a Mediterranean oak forest on soil properties influencing water infiltration. *J. Hydrol. Hydromech.* **2017**, *65*, 276–286. [\[CrossRef\]](#)
26. Startsev, A.D.; McNabb, D.H. Effects of skidding on forest soil infiltration in west-central Alberta. *Can. J. Soil Sci.* **2000**, *80*, 617–624. [\[CrossRef\]](#)
27. Hayashi, Y.; Ken'Ichirou, K.; Mizuyama, T. Changes in pore size distribution and hydraulic properties of forest soil resulting from structural development. *J. Hydrol.* **2006**, *331*, 85–102. [\[CrossRef\]](#)
28. Toriyama, J.; Ohta, S.; Araki, M.; Kosugi, K.; Nobuhiro, T.; Kabeya, N.; Shimizu, A.; Tamai, K.; Kanzaki, M.; Chann, S. Soil pore characteristics of evergreen and deciduous forests of the tropical monsoon region in Cambodia. *Hydrol. Process.* **2010**, *25*, 714–726. [\[CrossRef\]](#)
29. Perkins, K.S.; Nimmo, J.R.; Medeiros, A.C. Effects of native forest restoration on soil hydraulic properties, Auwahi, Maui, Hawaiian Islands. *Geophys. Res. Lett.* **2012**, *39*. [\[CrossRef\]](#)
30. Krauss, G.A. Die Sogenannten Bodenerkrankungen (Mit Vorweisung Natürlicher Waldbodenprofile). *Jahresber. Dtsch. Forstvereins.* **1928**, *328*, 121–156.
31. Kubiena, W.L. *The Soils of Europe: Illustrated Diagnosis and Systematics, with Keys and Descriptions for Easy Identification of the Most Important Soil Formations of Europe with Consideration of the Most Frequent Synonyms*; T. Murby & Co: London, UK, 1953.
32. Krauss, G.A.; Müller, K.; Gärtner, K. Standortsgemäße Durchführung der Abkehr von der Fichtenwirtschaft im Nordwestsächsischen Niederland (Mit grundsätzlichen Bemerkungen über “gleiartige” Bodenbildungen. *Thar. Forstl J.* **1939**, *90*, 481–715.
33. Schwärzel, K.; Punzel, J. Hood Infiltrometer-A New Type of Tension Infiltrometer. *Soil Sci. Soc. Am. J.* **2007**, *71*, 1438–1447. [\[CrossRef\]](#)
34. Reynolds, W.D.; Elrick, D.E. Determination of Hydraulic Conductivity Using a Tension Infiltrometer. *Soil Sci. Soc. Am. J.* **1991**, *55*, 633–639. [\[CrossRef\]](#)
35. Ankeny, M.D.; Ahmed, M.; Kaspar, T.C.; Horton, R. Simple Field Method for Determining Unsaturated Hydraulic Conductivity. *Soil Sci. Soc. Am. J.* **1991**, *55*, 467–470. [\[CrossRef\]](#)
36. Reynolds, W.D.; Bowman, B.T.; Brunke, R.R.; Drury, C.F.; Tan, C.S. Comparison of Tension Infiltrometer, Pressure Infiltrometer, and Soil Core Estimates of Saturated Hydraulic Conductivity. *Soil Sci. Soc. Am. J.* **2000**, *64*, 478–484. [\[CrossRef\]](#)
37. Bagarello, V.; Baiamonte, G.; Castellini, M.; Di Prima, S.; Iovino, M. A comparison between the single ring pressure infiltrometer and simplified falling head techniques. *Hydrol. Process.* **2014**, *28*, 4843–4853. [\[CrossRef\]](#)
38. Kosugi, K. Lognormal Distribution Model for Unsaturated Soil Hydraulic Properties. *Water Resour. Res.* **1996**, *32*, 2697–2703. [\[CrossRef\]](#)
39. Greenland, D.J. Soil Management and Soil Degradation. *Eur. J. Soil Sci.* **1981**, *32*, 301–322. [\[CrossRef\]](#)
40. Lenth, R.; Singmann, H.; Love, J.; Buerkner, P.; Herve, M. Emmeans: Estimated Marginal Means, Aka Least-Squares Means. *R Packag. Version* **2018**, *1*, 3.
41. Agnese, C.; Bagarello, V.; Baiamonte, G.; Iovino, M. Comparing Physical Quality of Forest and Pasture Soils in a Sicilian Watershed. *Soil Sci. Soc. Am. J.* **2011**, *75*, 1958–1970. [\[CrossRef\]](#)
42. Noguchi, S.; Tsuboyama, Y.; Sidle, R.C.; Hosoda, I. Morphological Characteristics of Macropores and the Distribution of Preferential Flow Pathways in a Forested Slope Segment. *Soil Sci. Soc. Am. J.* **1999**, *63*, 1413–1423. [\[CrossRef\]](#)
43. Hagedorn, F.; Bundt, M. The age of preferential flow paths. *Geoderma* **2002**, *108*, 119–132. [\[CrossRef\]](#)
44. Withington, J.M.; Reich, P.; Oleksyn, J.; Eissenstat, D.M. Comparisons of structure and life span in roots and leaves among temperate trees. *Ecol. Monogr.* **2006**, *76*, 381–397. [\[CrossRef\]](#)
45. Thomas, F.M. Vertical rooting patterns of mature *Quercus* trees growing on different soil types in northern Germany. *Plant Ecol.* **2000**, *147*, 95–103. [\[CrossRef\]](#)
46. Thomas, F.M.; Hartmann, G. Tree rooting patterns and soil water relations of healthy and damaged stands of mature oak (*Quercus robur* L. and *Quercus petraea* [Matt.] Liebl.). *Plant Soil* **1998**, *203*, 145–158. [\[CrossRef\]](#)
47. Schmid, I.; Kazda, M. Root distribution of Norway spruce in monospecific and mixed stands on different soils. *For. Ecol. Manag.* **2002**, *159*, 37–47. [\[CrossRef\]](#)